euronoise

The design and modelling of a lateral acoustic particle manipulator exhibiting quarter-wave operation

P. Glynne-Jones[a], M. Hill[a], N. R Harris[b], R. J Townsend[a] and S. K Ravula[c]

[a]University of Southampton, School of Engineering Sciences, University Road, SO17 1BJ Southampton, UK
[b]University of Southampton, Electronics and Computer Science, SO17 1BJ Southampton, UK
[c]Sandia National Laboratories, Eubank Blvd, Albuquerque, NM 87123, USA
p.glynne-jones@soton.ac.uk

Petersson et al. [Petersson et al., 2004] have demonstrated the operation of a half-wave acoustic particle manipulator, whose forces act in the plane of a silicon substrate. In a half-wave device particles are directed to the centre of a channel. Devices acting in plane have manufacturing advantages, and lend themselves to many microfluidic applications. We demonstrate, for the first time, such a device with a quarter-wave mode that is able to manipulate particles to the side of a channel. The design utilises resonant 'islands' to create the necessary acoustic boundary conditions. The device is conventionally milled in brass, permitting cheaper and quicker fabrication than in silicon. Finite element modelling is presented to elucidate the operation of the device. In contrast to essentially one-dimensional planar devices, the two-dimensional distribution of the velocity and pressure fields result in particles being constrained to lines within the channel.

1 Introduction

Acoustic radiation forces are a promising alternative to optical trapping as a means of manipulating micron-scale particles and biological cells [1]. Various topologies have been demonstrated, including: focussed ultrasound [2]; the use of two or more transducers to modulate the standing wave field [3]; the use of plate waves coupled into a containing fluid to excite the field [4]; layered resonators with a single transducer [5-7]; and channels etched into a substrate that support lateral acoustic modes, excited by a transducer attached to the back of the substrate [8]. The complex two-dimensional geometry of the latter design, has not been the subject of as much modelling as the others, and its exact mode of operation is not well understood. This lateral resonator configuration is explored here.

Whereas the existing designs produce half-wave resonators, we report here on some initial results from a new type of lateral quarter-wave particle manipulator. We also show how finite element analysis can be combined with Gor'kov's [9] equations for acoustic radiation force to predict the behaviour of this and other devices that cannot be approximated by one-dimensional models.

2 Device design

The basic design of the device substrate is shown in Figure 1. Two devices with varying depths of channel have been manufactured on the same brass substrate. Only the left hand device is tested and described in this paper. Each device is formed by milling three parallel grooves in the brass. The centre groove forms a fluid channel, while the function of the others is to provide suitable acoustic boundary conditions to their adjacent brass 'islands'. A PZT26 transducer (Ferroperm, 15mmx7mm, thickness 1mm) supplies excitation, and is glued with epoxy (Epotek 301 epoxy) to the underside of the channels. A glass microscope slide, 1.2mm thick, is clamped to the top of the brass to form a top surface for the fluid channel.

To form fluidic connections to the device, there are ports through the substrate (diameter 0.5mm). To the back of these holes, a ferrule (Upchurch P200) is glued using epoxy; to this 1cm of 1.6mm (inside diameter) silicone tubing is superglued – this forms a convenient low-pressure push-to-seal connection for 1.6mm (outer diameter) tubing.

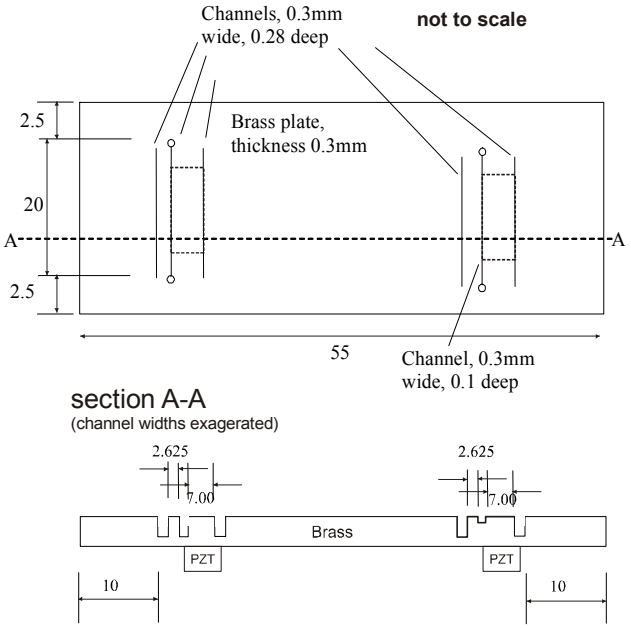

Figure 1: Substrate design (dimensions in mm)

The intended mode of operation of the device was to be similar in concept to more conventional layered quarter-wave acoustic particle manipulators [10, 11], with the thickness resonances replaced by lateral resonances excited by the PZT. However, finite element analysis, below, suggests that surface waves dominate the behaviour of the device in an unexpected way.

3 Finite Element Analysis

The design of acoustic particle manipulation devices has generally been performed using one-dimensional approaches [5, 7]. Finite Element models have been described by Neild et al. [12] and Townsend et al. [13], and this work extends that of Townsend, incorporating a finite element representation of the transducer and using the results to visualise the force distribution in two-dimensions. Even in layered resonator designs which are most suited to a one-dimensional approach, significant lateral variations in acoustic radiation forces can be observed [13], which finite element analysis could be used to model.

A full verification of this Finite Element approach is beyond the scope of this paper, but a future paper will present results verifying the finite element model to ensure that its results are reliable – for now, Figure 2 presents some initial verification: it is based on the layered resonator described by Glynne-Jones et al [14], and compares results from a finite element model with a transmission line model described by Hill [**7**], but incorporating the KLM piezoelectric circuit model [15] to extend the region of

validity beyond the transducer's first resonance. The finite element model is based in ANSYS, and uses a strip of FLUID29 (2-D harmonic acoustic) elements; lateral boundary conditions to model an infinite plane; carrier and reflector layers are represented by 2-D structural solid elements, PLANE42; and the PZT by the piezoelectric formulation of the 2-D Coupled-Field Solid PLANE13. Varying the parameters of the transmission line model, it is found that for the parameters considered here, the air beyond the reflector and transducers has little effect on the energy density profile, and is not included in the ANSYS model. The acoustic fluid elements are not formulated to allow any fluid damping in the fluid body, which makes predictions of acoustic amplitudes less accurate, particularly for half-wave devices where the fluid damping is important, however in the future, other element types such as FLUID79 which can include fluid damping will be explored. All materials data is taken from manufacturers' data tables.

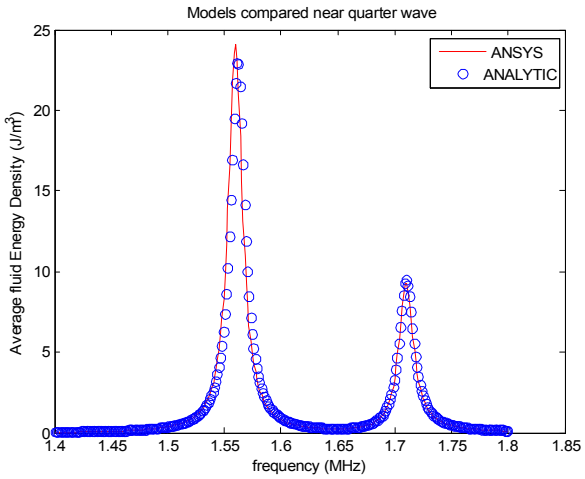

Figure 2: Comparing ANSYS model to transfer impedance model

In order to calculate the acoustic radiation force on a particle at points within the fluid, the following equations derived by Gor'kov [9] are used: The acoustic radiation force (a time averaged quantity) is given by

$$\langle F(r)\rangle = -\nabla\langle\phi(r)\rangle \qquad (1)$$

where the force potential, $\langle\phi(r)\rangle$, is given by

$$\langle\phi(r)\rangle = -V\left[\frac{3(\lambda-1)}{2\lambda+1}\langle\overline{E}_{kin}(r)\rangle - \left(1-\frac{1}{\sigma^2\lambda}\right)\langle\overline{E}_{pot}(r)\rangle\right] \qquad (2)$$

Where λ is the ratio of particle density to fluid density, σ the ratio of speed of sound in the particle to that in the fluid, V the particle volume, and $\langle\overline{E}_{kin}(r)\rangle$ and $\langle\overline{E}_{pot}(r)\rangle$ the time averaged kinetic and potential energy densities of the sound wave in the fluid. For a harmonically varying sound field, where the fluid particle velocity, u, has amplitude U and fluid pressure, p, has amplitude P, these can be calculated [16] as

$$\langle\overline{E}_{kin}(r)\rangle = \frac{1}{T}\int_0^T E_{kin}(r) = \frac{1}{T}\int_0^T \frac{1}{2}\rho_0 u^2 = \frac{1}{4}\rho_0 U^2 \qquad (3)$$

and

$$\langle\overline{E}_{pot}(r)\rangle = \frac{1}{T}\int_0^T E_{pot}(r) = \frac{1}{T}\int_0^T \frac{1}{2}\frac{p^2}{\rho_0 c^2} = \frac{1}{4}\frac{P^2}{\rho_0 c^2} \qquad (4)$$

Where T is the period of the harmonic wave, ρ_0 is the density of the fluid, and c the speed of sound in the fluid.

Post processing of the finite element results, allows these equations to be implemented. Plotting the acoustic force potential, $\langle\phi(r)\rangle$, is a convenient way of visualising the acoustic forces. A particle will tend to move towards regions where $\langle\phi(r)\rangle$ is low with a force proportional to the spacings of plotted contour lines.

4 Device explored

As an accurate model of the experimental device, the model that follows is weak as the boundary conditions are significantly simplified. However, the modelled results are useful as they demonstrate the likely mode of operation of the device, and show some features that are found experimentally.

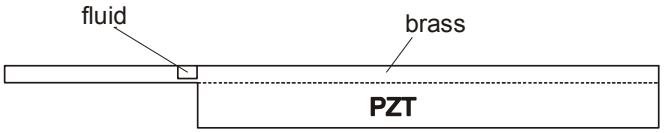

Figure 3: Areas modelled in finite element model

The outline of the model is shown in Figure 3 – it only extends as far as the edges of the brass 'islands'. The glass slide covering the channel and brass is not modelled, since it is only clamped with sufficient force to hold it in place. The surface waves found in the results that follow are likely to be attenuated by the glass and the resulting squeeze-film layer of air, but it seems reasonable to use this model to give an indication of the type of behaviour that could be expected. To produce more useful devices in future, the glass layer would need to be bonded more effectively to the underlying layers. The top of the fluid surface is modelled as an acoustically reflecting boundary (IMPD flag set to 1), and element types used as described above. Mesh sizes are set to 10µm in the fluid channel, and a maximum of 40µm in the brass, corresponding to 0.0092λ and 0.012λ respectively at 1.37MHz. A voltage boundary condition is applied across the piezoelectric PZT, to apply the excitation.

Figure 4 plots the resulting average energy density in the fluid channel versus excitation frequency for a 10Vpp excitation voltage. It can be seen that there are several maxima, each of which produce different acoustic force distributions within the fluid. We will only describe here the one found at 1.458MHz, as it exhibits quarter wave type behaviour. The acoustic force potential at this frequency is plotted in Figure 5. It can be seen that particles (of positive acoustic contrast factor) are driven towards both the upper

right and, with less force, to the lower left corners of the channel. Examining the element displacement data, it is found that the majority of the structural energy is carried in flexural Lamb-type waves (this is also true of the other peaks in Figure 4). Figure 6 shows a plot of the real part of the nodal displacements, with the displacement scaled by a factor of 7000 to make it clearer.

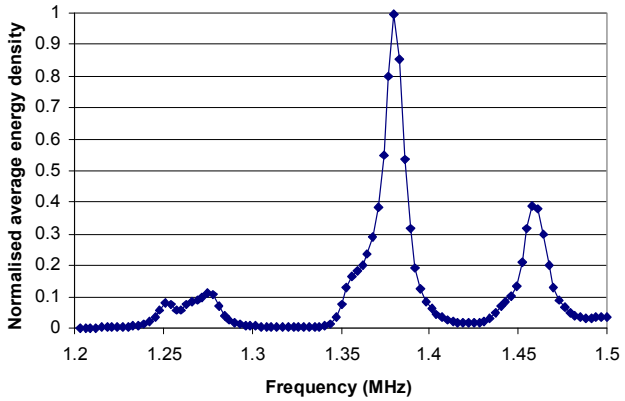

Figure 4: Average Energy density in fluid channel versus frequency

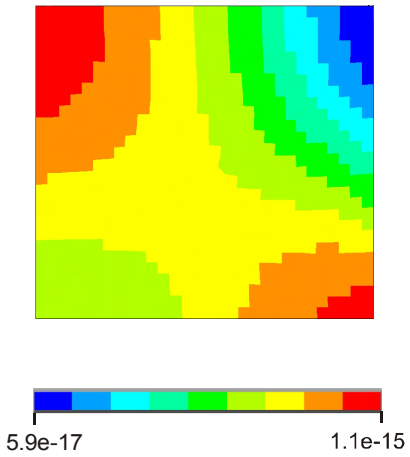

Figure 5: Modelled acoustic force potential (Nm), f=1.458MHz

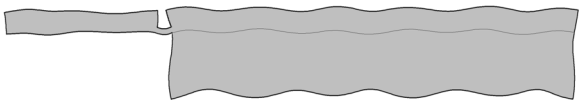

Figure 6: Exagerated displacement plot at 1.458MHz

A dilute solution of fluorescent 10µm polystyrene beads (Polysciences Inc., Fluoresbrite microspheres #19096) was flowed down the channel for 2 minutes, with the transducer driven at 19Vpp and a frequency of 1.37MHz. Figure 7 shows an image of the device after this time [a movie of the device in action is available on the conference CD]. During this time, beads could be observed flowing down the channel, and moving laterally across the flow under the action of the acoustic radiation force. Upon reaching the channel walls, the beads became stuck; the distribution of beads shows that, as in the model, the force potential drives beads towards two different points. The velocity of the beads as they moved towards the stronger of the two trapping locations was of the order of 100-200µm/s, corresponding (by assuming viscous Stoke's drag) to an acoustic radiation forces of around 10-20pN

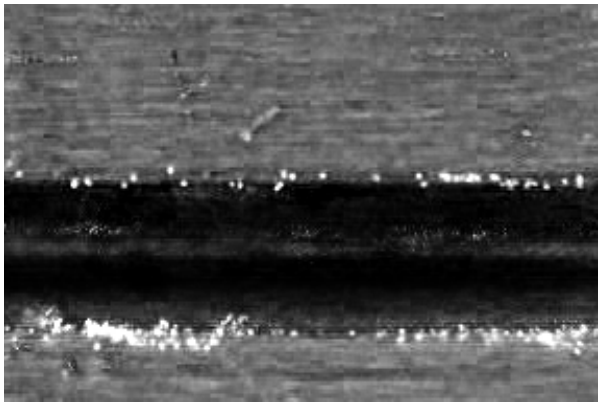

Figure 7: Image of bead distribution after 2 mins of device operation at 1.37MHz. The dark region is the fluid channel.

5 Conclusions

A novel device that uses surface acoustic waves to form boundary conditions for a laterally acting quarter-wave acoustic particle manipulator has been presented. The mode of operation of the device has been elucidated by Finite Element analysis in conjunction with the Gor'kov equations [9] to relate the properties of the acoustic field to its corresponding radiation force pattern.

Initial experimental findings support the model, but further experiments are required to characterise this device more accurately, and to develop a model with boundary conditions that match the device more accurately.

References

[1] M. Hill and N. R. Harris, "Ultrasonic Particle Manipulation," in *Microfluidic Technologies for Miniaturized Analysis Systems*, S. Hardt and F. Schönfeld, Eds.: Springer US, 2007, pp. 357-392.

[2] M. Wiklund, J. Toivonen, M. Tirri, P. Hanninen, and H. M. Hertz, "Ultrasonic enrichment of microspheres for ultrasensitive biomedical analysis in confocal laser-scanning fluorescence detection," *Journal Of Applied Physics,* vol. 96, pp. 1242-1248, 2004.

[3] Y. Abe, M. Kawaji, and T. Watanabe, "Study on the bubble motion control by ultrasonic wave," *Experimental Thermal and Fluid Science,* vol. 26, pp. 817-826, 2002.

[4] A. Neild, S. Oberti, F. Beyeler, J. Dual, and B. J. Nelson, "A micro-particle positioning technique combining an ultrasonic manipulator and a microgripper," *Journal of Micromechanics And Microengineering,* vol. 16, pp. 1562-1570, 2006.

[5] M. Gröschl, "Ultrasonic separation of suspended particles - Part I: Fundamentals," *Acustica,* vol. 84, pp. 432-447, 1998.

[6] J. J. Hawkes and W. T. Coakley, "Force field particle filter, combining ultrasound standing waves and laminar flow," *Sensors and Actuators B-Chemical,* vol. 75, pp. 213-222, 2001.

[7] M. Hill, Y. Shen, and J. J. Hawkes, "Modelling of layered resonators for ultrasonic separation.," *Ultrasonics,* vol. 40, pp. 385-92, 2002.

[8] F. Petersson, A. Nilsson, C. Holm, H. Jonsson, and T. Laurell, "Separation of lipids from blood utilizing ultrasonic standing waves in microfluidic channels," *Analyst,* vol. 129, pp. 938-943, 2004.

[9] L. P. Gor'kov, "On the forces acting on a small particle in an acoustical field in an ideal fluid," *Sov. Phys. Dokl.,* vol. 6, pp. 773-5, 1962.

[10] M. Hill, "The selection of layer thicknesses to control acoustic radiation force profiles in layered resonators," *Journal of the Acoustical Society of America,* vol. 114, pp. 2654-2661, 2003.

[11] S. P. Martin, R. J. Townsend, L. A. Kuznetsova, K. A. J. Borthwick, M. Hill, M. B. McDonnell, and W. T. Coakley, "Spore and micro-particle capture on an immunosensor surface in an ultrasound standing wave system," *Biosensors and Bioelectronics,* vol. 21, pp. 758-767, 2005.

[12] A. Neild, S. Oberti, A. Haake, and J. Dual, "Finite element modeling of a microparticle manipulator," *Ultrasonics,* vol. 44, pp. e455-e460, 2006.

[13] R. J. Townsend, M. Hill, N. R. Harris, and N. M. White, "Investigation of two-dimensional acoustic resonant modes in a particle separator," *Ultrasonics,* vol. 44, pp. e467-e471, 2006.

[14] P. Glynne-Jones, F. Zhang, L. Dong, J. S. Wilkinson, T. Melvin, N. R. Harris, R. J. Townsend, and M. Hill, "An integrated multimodal acoustic particle manipulator and waveguide sensor for the detection of DNA," *Presented at this conference*.

[15] Krimholt.R, D. A. Leedom, and G. L. Matthaei, "New Equivalent Circuits for Elementary Piezoelectric Transducers," *Electronics Letters,* vol. 6, p. 398, 1970.

[16] L. E. Kinsler, A. E. Frey, A. B. Coppens, and J. V. Saunders, *Fundamentals of acoustics*, 3rd ed. New York: Wiley, 1982.